Multi-agent system-based event-triggered hybrid control scheme for energy internet

Dou, Chunxia; Yue, Dong; Han, Qing Long; Guerrero, Josep M.

Published in:
IEEE Access

DOI (link to publication from Publisher):
10.1109/ACCESS.2017.2670778

Publication date:
2017

Document Version
Publisher's PDF, also known as Version of record

IEEE Access
Multidisciplinary ⋮ Rapid Review ⋮ Open Access Journal

Received December 16, 2016, accepted January 14, 2017, date of publication February 17, 2017, date of current version March 28, 2017.

Digital Object Identifier 10.1109/ACCESS.2017.2670778

Multi-Agent System-Based Event-Triggered Hybrid Control Scheme for Energy Internet

CHUNXIA DOU[1,2], DONG YUE[1], (Senior Member, IEEE), QING-LONG HAN[3], (Senior Member, IEEE), AND JOSEP M. GUERRERO[4], (Fellow, IEEE)

[1]Institute of Advanced Technology, Nanjing University of Posts and Telecommunications, Nanjing 210023, China
[2]Institute of Electrical Engineering, Yanshan University, Qinhuangdao 066004, China
[3]School of Software and Electrical Engineering, Swinburne University of Technology, Melbourne, VIC 3122, Australia
[4]Department of Energy Technology, Aalborg University, 9220 Aalborg East, Denmark

Corresponding author: D. Yue (medongy@vip.163.com)

This work was supported in part by the National Natural Science Foundation of China under Grant 61573300 and Grant 61533010, in part by the Hebei Provincial Natural Science Foundation of China under Grant E2016203374, in part by the Primary Research & Development Plan of Jiangsu Province under Grant BE2016184, and in part by the Australian Research Council Discovery Project under Grant DP160103567.

ABSTRACT This paper is concerned with an event-triggered hybrid control for the energy Internet based on a multi-agent system approach with which renewable energy resources can be fully utilized to meet load demand with high security and well dynamical quality. In the design of control, a multi-agent system framework is first constructed. Then, to describe fully the hybrid behaviors of all distributed energy resources and logical relationships between them, a differential hybrid Petri-net model is established, which is an original work. The most important contributions based on this model propose four types of event-triggered hybrid control strategies whereby the multi-agent system implements the hierarchical hybrid control to achieve multiple control objectives. Finally, the effectiveness of the proposed control is validated by means of simulation results.

INDEX TERMS Energy Internet, multi-agent system, hybrid control, event-triggered control, differential hybrid Petri-net.

I. INTRODUCTION

The energy internet is an emerging information and physical fusion network, which consists of two main layers: (i) an upper-layer Internet, and (ii) a lower-layer energy network [1]. The lower layer integrates various kinds of distributed renewable energy resources (RERs), distributed storage devices and loads. It is usually connected to a main grid through a bi-directional grid-connected converter (GCC), which forms a resource-grid-load-storage interconnected energy network. In comparison with a microgrid, the lower-layer energy network integrates resource-grid-load-storage in a more loose way. With the support of the upper-layer Internet, more convenient interactions between the distributed units can be realized in energy internet, which can guarantee a realization of frequent access or exit of those units. The structure of energy internet appears time-varying performance with multi-mode switching characteristics [2]–[4]. From the whole system point of view, the energy internet has a typical characteristic of a complex hybrid system, and thus its control presents even greater challenge [5], [6].

One of the main envisioned conceptions of the energy internet is to make full use of RERs to meet the load demand with high reliability and well dynamic quality. To achieve these objectives, an effective control mechanism should be introduced by fully utilizing information from the upper-layer Internet and taking the hybrid characteristic of the energy internet into account. Although much attention has been paid to the construction of the energy internet in recent years, there are only a few results available in the existing literature on the study of control of the energy internet. As mentioned above, the energy network is the main part of the energy internet. In the past several decades, several control approaches about the energy network with traditional communication networks have been investigated. However, the control schemes proposed in most of the existing references are dynamical

regulation without paying sufficient attention to the treatment of the switching behavior of the energy network [9]–[11]. In [9], an energy management issue was addressed by means of the switching control for four kinds of operation modes. In [10] and [11], MAS based switching control was proposed for storage devices by using logic judgments and fuzzy-logic-rules, respectively. From the existing references mentioned above, it can be seen that the study of control by considering the switching performance of the energy network is primary and still in its infancy. Furthermore, the existing control scheme for the energy network often adopts a hierarchical control structure [4], [7], [8] due to the limitation of the traditional communication infrastructure.

In this paper, by making full use of the upper-layer Internet and considering more prominent hybrid characteristic of the energy internet, we propose a hybrid control scheme with the following features: (i) mode switching, which can switch operation modes of the resource-grid-load-storage in a coordinated way to guarantee power supply with high security; (ii) dynamical regulation, which can continuously regulate each unit system to guarantee power supply with well dynamic quality; and (iii) widely real-time interactions, which depend on the upper-layer Internet. The main contributions of this paper are summarized as follows: (i) three levels of the multi-agent system (MAS) is constructed to carry out the hierarchical hybrid control so as to achieve multiple control objectives; and (ii) an event-triggered hybrid control scheme is designed based on a differential hybrid Petri-net (DHPN) model.

In comparison with some existing results [9]–[11], the advantages of the proposed control scheme are as follows: (i) the three levels of the MAS can take full use of information from the upper-layer Internet to intelligently carry out hierarchical hybrid control in a distributed coordinated way, and thus the multiple control objectives are achieved simultaneously; (ii) the interaction topology of the MAS is easy to be dynamically re-constructed when dealing with ''plug and play'' of units in the system. In this sense, the proposed control scheme is very flexible and scalable; (iii) the hybrid control strategies are designed as event-triggered functions (ETFs) or constraint violation functions (CVFs) fully depending on the logical relationship between the resources-grid-load- storage, which acts on all DERs and load demand side. In this sense, the event-triggered hybrid control scheme has the strong coordinating and regulating ability to cope with the effect of strong disturbances; and (iv) compared with the result in [12], this paper pays more attention to the hierarchical switching of RERs and hierarchical load shedding, and thus the proposed control scheme can make full use of RERs to meet the load demand in a more reasonable way.

The rest of this paper is organized as follows. Section II discusses an MAS based control scheme. A DHPN model is built in Section III. Section IV focuses on four kinds of hybrid control strategies. The control performance is verified in Section V. Section VI concludes this paper.

II. AN MAS BASED CONTROL SCHEME

A group of photovoltaic/wind turbine (PV/WT) combined RERs, storage devices and loads are firstly respectively connected to a common DC bus in a loose way, and then connected with an AC main grid through a GCC, which constitutes a resource-grid-load-storage interconnected energy network. The energy network combines with the upper-layer Internet to form the energy internet.

Three levels of the MAS are firstly constructed to carry out the hierarchical hybrid control so as to achieve multiple control objectives, whose structure can be seen in Fig. 1. (i) The GCC between the energy network and the main grid is associated with the first-level agent, which is mainly responsible for switching control of the GCC to guarantee operative security of the whole energy network. (ii) According to operation modes of the GCC, the second-level agent is employed to implement the switching control among resource-load-storage in a coordinated way, which is of an advantage of making full use of RERs to meet the load demand with high security. (iii) Each RER unit, storage unit or load demand side is also associated with the third-level unit control agent, which implements local switching control and distributed dynamic control to guarantee security and stability of its unit system.

The three levels of agents interact with each other through the upper-layer Internet by using the following two modes: (i) a master-slave interactive mode among different levels of agents. It means that the first-level agent has a priority over other agents, and the second-level agent has a priority over all the third-level unit agents; and (ii) a non master-slave interactive mode among third-level unit agents. That is, all third-level unit agents interact with each other in an equal way.

III. THE MODELING OF THE ENERGY INTERNET

As one of the best modeling methods for a complex hybrid system [13], [14], a DHPN model is employed to describe the hybrid behaviors of all DERs and logical relationships between them. Corresponding to the Fig. 1, the DHPN model consists of five subsystems as shown in Fig. 2, where RERs are divided into PV and WT units. The DHPN model is defined by a 7-tuple (PD, TD, PDF, TDF, AN, Γ, M0) set, where the descriptions regarding places (i.e. PD, PDF) and transitions (i.e. TD, TDF) are given in Tables 3-6

$A_N \subseteq ((P_D \times T_D) \cup (T_D \times P_D)) \cup ((P_D \times T_{DF}) \cup (T_{DF} \times P_D))$ is a set of arcs;

$\Gamma \in \{d_{TG1}, d_{TG2}, \ldots, d_{TLrn},\}$ is a timing map for all the discrete transients, which defines the triggered response time of all the discrete transients;

$M_0 \in \{M_{G0}, M_{B0}, M_{P0}, M_{W0}, M_{L0}\}$ is the initial marking, which defines the initial operation mode of resource- grid-load-storage.

The initial marking is described as ''discrete place with a token (black dot)'' in Fig. 2. When the operation mode is switched, the token is transmitted into corresponding posterior place from the initial place. If a unit system is in Pi

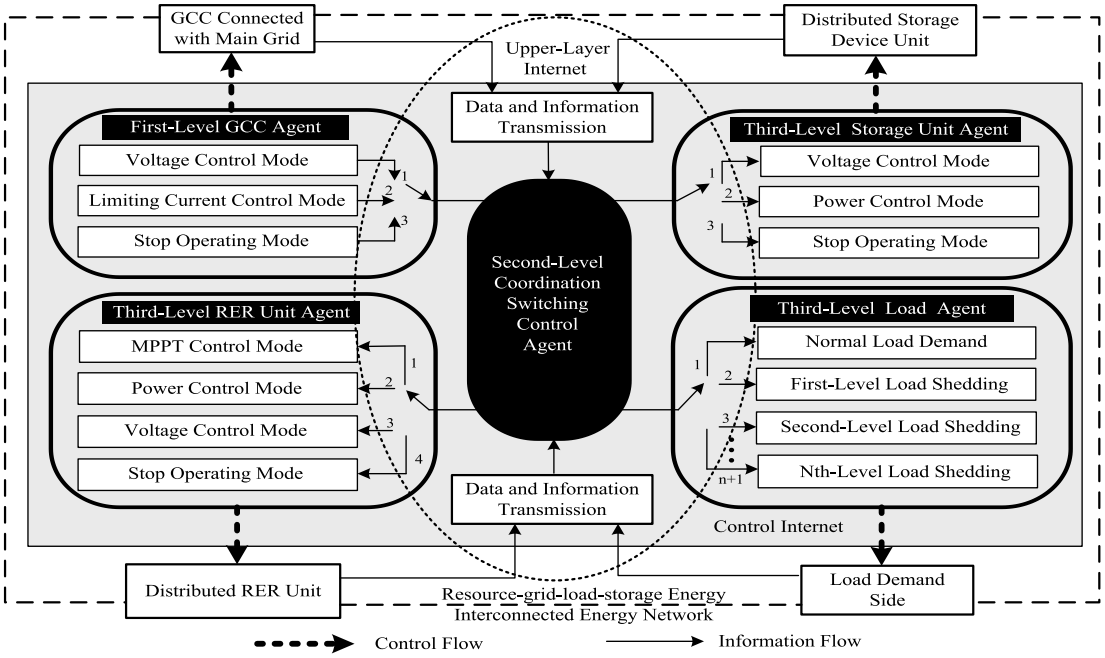

FIGURE 1. MAS based control scheme for the energy internet.

operation mode, then logical function F(Pi) of Pi is defined as "1"; otherwise, F(Pi) is "0". At any instant, in each subsystem, there is only one logical function being "1", and others are "0".

According to the switching principle of the DHPN model, only when one discrete (or differential) transition is triggered, the corresponding operation mode (or control mode) associated with the transition may be switched. Therefore, to switch the operation modes (or control modes) in a reasonable way, all transitions should be triggered by means of a designed event-triggered control strategy. In this paper, corresponding to different control objectives, an even-triggered hybrid control scheme includes: (i) the switching control strategy in the first-level agent, which is designed as a set of ETFs to intelligently switch operation mode of GCC, and is described as "—◇" in Fig. 2; (ii) the coordinated switching control strategy in the second-level agent, which is also designed by a set of ETFs to switch operation modes of resources-load-storage in a coordinated way, and is described as "➔" in Fig. 2; (iii) the local switching control strategy in each third-level unit agent, which is designed as a set of event-triggered CVFs to locally switch the operation mode of respective unit system, is described as "—▷" in Fig. 2; and (iv) the distributed dynamic control strategy in each third-level unit agent, which is designed to guarantee dynamic stability of respective unit system, is described as "┈┈▷" in Fig. 2.

IV. AN EVENT-TRIGGERED HYBRID CONTROL SCHEME

A. THE SWITCHING CONTROL STRATEGY FOR THE GCC UNIT

The switching control strategy "—◇" is designed as a set of ETFs associated with transitions based on the following triggered principle of DHPN mode: (i) once an ETF is activated (i.e. becomes logic "1"), it will trigger the connected transition; (ii) at the moment, if predecessor place of the transition has token, then the token will be transmitted into its posterior place; (iii) as a result, the corresponding operation mode is switched.

In the first-level GCC agent, the ETFs associated with TG1-TG4 are designed as follows:

$$\begin{aligned} \mathrm{ETF}(\mathrm{T_{G1}}) = {} & \mathrm{Sgn}[\max\{(I_g(t) - I_{g,\max}), 0\}] \\ & \mathrm{Sgn}[\max\{\Delta\,|U_d(t)| - 0.05, 0\}] \\ & \times[1(t) - 1(t - d_{\mathrm{TG1}})] \end{aligned} \tag{1}$$

$$\begin{aligned} \mathrm{ETF}(\mathrm{T_{G2}}) = {} & \mathrm{Sgn}[\max\{(I_{g,\max} - I_g(t)), 0\}] \\ & \times[1(t) - 1(t - d_{\mathrm{TG2}})] \end{aligned} \tag{2}$$

$$\mathrm{ETF}(\mathrm{T_{G3}}) = \bar{F}(t)\,[1(t) - 1(t - d_{\mathrm{TG3}})] \tag{3}$$

$$\mathrm{ETF}(\mathrm{T_{G4}}) = F(t)[1(t) - 1(t - d_{\mathrm{TG4}})] \tag{4}$$

where $\Delta U_d(t) = U_{ref}(t) - U_d(t)$; $\Delta U_d(t)$ is defined as the DC bus voltage deviation; $U_d(t)$ is a real per unit value of the DC bus voltage; $U_{ref}(t)$ is its reference per unit value; and 0.05 is defined as its maximum allowable deviation. In addition, $F(t)$ is a fault logical function ($F(t)$ is "1" if the main grid occurs fault, otherwise it is "0"); $\bar{F}(t)$ is an inverse function of $F(t)$; Sgn(•) is a sign function; $1(t)$ is a unit step function; $I_g(t)$ is the GCC current, and $I_{g.\max}$ is its maximum limiting value; d_{TG1} is the triggered time corresponding to TG1, and d_{TG2}, d_{TG3} and d_{TG4} are defined in a similar way.

Taking Eq.(1) as an example, the design process is explained as follows. When $I_g(t) > I_{g.\max}$ or $\Delta\,|U_d(t)| > 0.05$, ETF(TG1) is activated (i.e. becomes logic "1"), and then triggers the connected transition TG1 for d_{TG1} duration.

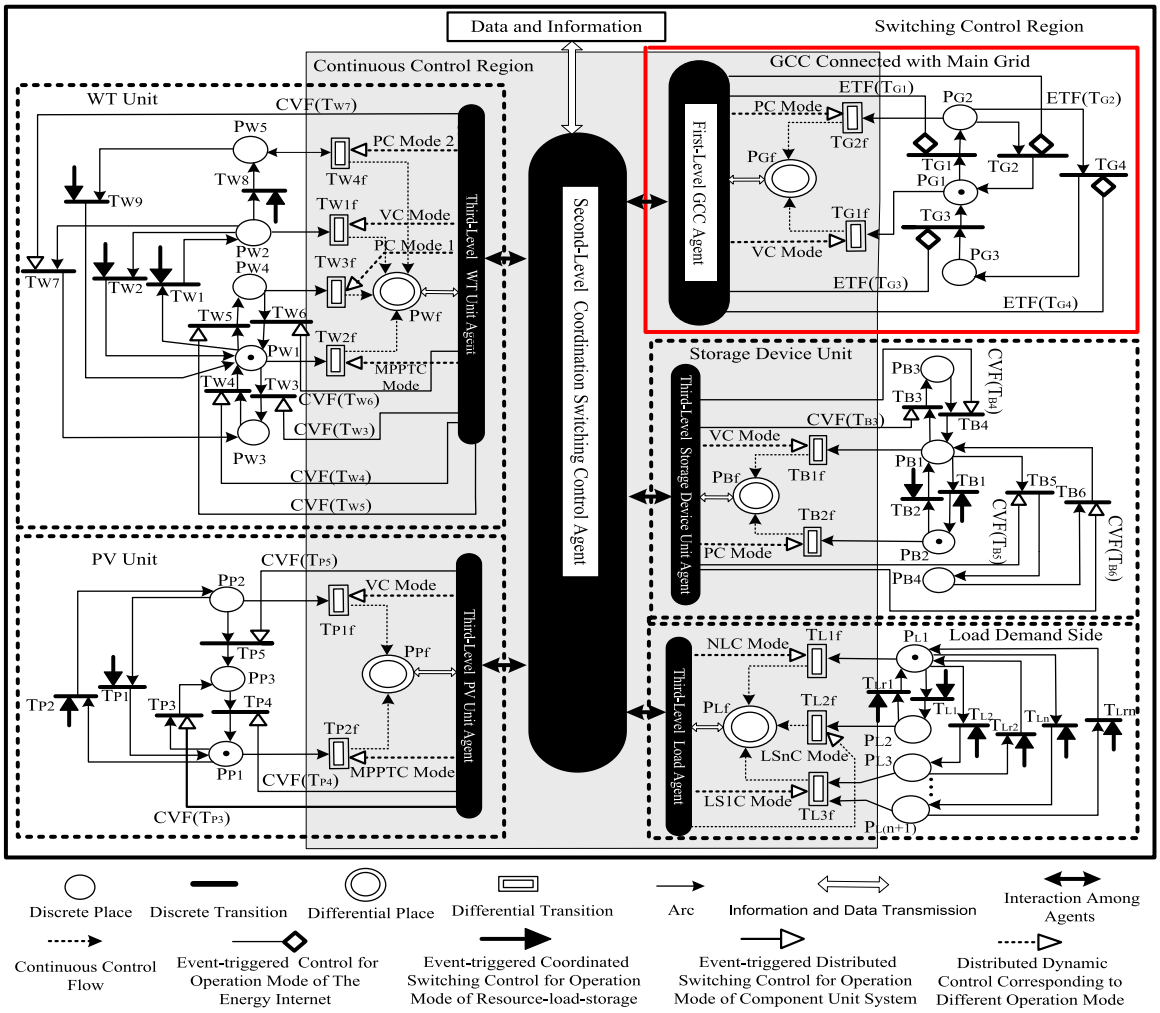

FIGURE 2. Event-triggered hybrid control strategies based on the DHPN model.

As a result, the GCC unit is switched from PG1 (i.e. voltage control mode) to PG2 (i.e. power control mode).

By means of the above switching control strategy, the control modes of GCC can be intelligently switched to ensure operative security of the interconnected energy network.

B. THE COORDINATED SWITCHING CONTROL STRATEGY

According to the following logical switching principles, the coordinated switching control strategy "→" is also designed as a set of ETFs associated with transition.

1) HIERARCHICAL LOAD SHEDDING

The events are given as follows:

(a) When a main grid fault occurs, the energy network will be switched to an islanded mode.

(b) The battery stops operating because of its lower S_{soc} (t) than 0.4S max (i.e. minimum state of charge).

(c) $0.1 \leq -\Delta U_d(t) \leq 0.15$, and the duration exceeds $\Delta T_1 > 0$.

(d) $0.1 \leq -\Delta U_d(t) \leq 0.2$, and the duration exceeds $\Delta T_2 > \Delta T_1 > 0$.

(e) $0.1 \leq -\Delta U_d(t) \leq 0.25$, and the duration exceeds $\Delta T_3 > \Delta T_2 > 0$.

The Switching Principle: If the events (a), (b) and (c) occur simultaneously, then the second-level agent informs the load agent to execute first-grade load shedding. If the events (a), (b) and (d) occur simultaneously, then the load agent implements second-grade load shedding. If the events (a), (b) and (e) occur simultaneously, then the load agent implements third-grade load shedding, and so on.

2) THE HIERARCHICAL SWITCHING CONTROL OF RERs

The events are defined as follows:

(a) When a main grid fault occurs, the energy network will be switched to an islanded mode.

(b) The battery stops operating because of its higher $S_{soc}(t)$ than 0.9 S_{max} (i.e. maximum state of charge).

(c) The voltage deviation is larger than and equal to 0.1, hat is $\Delta U_d(t) \geq 0.1$.

The Switching Principle: If the three events occur simultaneously, then the second-level agent informs the PV unit

agent to switch to the voltage control mode. If the three events still exist, the second-level agent informs the WT unit agent to switch to the voltage control mode. Finally, if three events still exist, then the WT unit agent switches its unit to the power control mode again in order to decrease the output power.

According to the above switching principle and triggered principle of DHPN mode, the ETFs regarding the coordinated switching control strategy are designed as follows

$$\mathrm{ETF}(\mathrm{T_{B2}}) = [\mathrm{F(P_{G2})} + \mathrm{F(P_{G3})}]\mathrm{F(P_{B2})}\,\Phi(\mathrm{T_{B2}}) \tag{5}$$

$$\mathrm{ETF}(\mathrm{T_{B1}}) = \mathrm{F(P_{G1})F(P_{B1})}\Phi(\mathrm{T_{B1}}) \tag{6}$$

$$\begin{aligned}\mathrm{ETF}(\mathrm{T_{L1}}) = {} & \mathrm{F(P_{G3})F(P_{B3})F(P_{L1})} \\ & \mathrm{Sgn}[\max\{(-\Delta U_d(t) - 0.1), 0\}] \\ & \mathrm{Sgn}[\max\{(0.15 + \Delta U_d(t)), 0\}] \\ & \mathrm{Sgn}[\max\{(-\Delta U_d(t - \Delta T_1) - 0.1), 0\}] \\ & \mathrm{Sgn}[\max\{(0.15 + \Delta U_d(t - \Delta T_1)), 0\}]\Phi(\mathrm{T_{L1}})\end{aligned} \tag{7}$$

$$\begin{aligned}\mathrm{ETF}(\mathrm{T_{L2}}) = {} & \mathrm{F(P_{G3})F(P_{B3})F(P_{L1})} \\ & \mathrm{Sgn}[\max\{(-\Delta U_d(t) - 0.1), 0\}] \\ & \mathrm{Sgn}[\max\{(0.2 + \Delta U_d(t)), 0\}] \\ & \mathrm{Sgn}[\max\{(-\Delta U_d(t - \Delta T_2) - 0.1), 0\}] \\ & \mathrm{Sgn}[\max\{(0.2 + \Delta U_d(t - \Delta T_2)), 0\}]\Phi(\mathrm{T_{L2}})\end{aligned} \tag{8}$$

$$\begin{aligned}\mathrm{ETF}(\mathrm{T_{Ln}}) = {} & \mathrm{F(P_{G3})F(P_{B3})F(P_{L1})} \\ & \mathrm{Sgn}[\max\{(-\Delta U_d(t) - 0.1), 0\}] \\ & \mathrm{Sgn}[\max\{(0.15 + (n-1)0.05 + \Delta U_d(t)), 0\}] \\ & \mathrm{Sgn}[\max\{(0.15 + (n-1)0.05 \\ & \qquad + \Delta U_d(t - \Delta T_n)), 0\}]\Phi(\mathrm{T_{Ln}}) \\ & \mathrm{Sgn}[\max\{(-\Delta U_d(t - \Delta T_n) - 0.1), 0\}]\end{aligned} \tag{9}$$

$$\begin{aligned}\mathrm{ETF}(\mathrm{T_{Lr1}}) = {} & \mathrm{F(P_{G1})F(P_{B2})F(P_{L2})} \\ & \mathrm{Sgn}[\max\{(0.05 + \Delta U_d(t)), 0\}] \\ & \mathrm{Sgn}[\max\{(0.05 + \Delta U_d(t - \Delta t_1)), 0\}]\Phi(\mathrm{T_{Lr1}})\end{aligned} \tag{10}$$

$$\begin{aligned}\mathrm{ETF}(\mathrm{T_{Lr2}}) = {} & \mathrm{F(P_{G1})F(P_{B2})F(P_{L3})} \\ & \mathrm{Sgn}[\max\{(0.05 + \Delta U_d(t)), 0\}] \\ & \mathrm{Sgn}[\max\{(0.05 + \Delta U_d(t - \Delta t_2)), 0\}]\Phi(\mathrm{T_{Lr2}})\end{aligned} \tag{11}$$

$$\begin{aligned}\mathrm{ETF}(\mathrm{T_{Lrn}}) = {} & \mathrm{F(P_{G1})F(P_{B2})F(P_{L(n+1)})} \\ & \mathrm{Sgn}[\max\{(0.05 + \Delta U_d(t)), 0\}] \\ & \mathrm{Sgn}[\max\{(0.05 + \Delta U_d(t - \Delta t_n)), 0\}] \\ & \times[1(t) - 1(t - d_{\mathrm{TLr1}})]\end{aligned} \tag{12}$$

$$\begin{aligned}\mathrm{ETF}(\mathrm{T_{P2}}) = {} & \mathrm{F(P_{G3})F(P_{B4})F(P_{P1})} \\ & \mathrm{Sgn}[\max\{(\Delta U_d(t) - 0.1), 0\}]\Phi(\mathrm{T_{P2}})\end{aligned} \tag{13}$$

$$\begin{aligned}\mathrm{ETF}(\mathrm{T_{P1}}) = {} & \{\mathrm{F(P_{G3})F(P_{B1})F(P_{P2})} + \mathrm{F(P_{G1})F(P_{B2})F(P_{P2})}\} \\ & \times\Phi(\mathrm{T_{P1}})\end{aligned} \tag{14}$$

$$\begin{aligned}\mathrm{ETF}(\mathrm{T_{W1}}) = {} & \mathrm{F(P_{G3})F(P_{B4})F(P_{P2})F(P_{W1})} \\ & \mathrm{Sgn}[\max\{(\Delta U_d(t) - 0.1), 0\}]\Phi(\mathrm{T_{W1}})\end{aligned} \tag{15}$$

$$\begin{aligned}\mathrm{ETF}(\mathrm{T_{W2}}) = {} & \{\mathrm{F(P_{G3})F(P_{B1})F(P_{W2})} + \mathrm{F(P_{G1})F(P_{B2})F(P_{W2})}\} \\ & \times\Phi(\mathrm{T_{W2}})\end{aligned} \tag{16}$$

$$\begin{aligned}\mathrm{ETF}(\mathrm{T_{W8}}) = {} & \mathrm{F(P_{G3})F(P_{B4})F(P_{P2})F(P_{W2})} \\ & \mathrm{Sgn}[\max\{(\Delta U_d(t) - 0.1), 0\}]\Phi(\mathrm{T_{W8}})\end{aligned} \tag{17}$$

$$\begin{aligned}\mathrm{ETF}(\mathrm{T_{W9}}) = {} & \{\mathrm{F(P_{G3})F(P_{B1})F(P_{W5})} + \mathrm{F(P_{G1})F(P_{B2})F(P_{W5})}\} \\ & \times\Phi(\mathrm{T_{W9}})\end{aligned} \tag{18}$$

where $\Phi\ (\mathrm{T_D}) = 1(t) - 1(t - d_{\mathrm{TD}})$ is the triggered time, and $T_D \in \{\mathrm{T_{G1}}, \ldots, \mathrm{T_{G4}}, \mathrm{T_{B1}}, \ldots, \mathrm{T_{B6}}, \mathrm{T_{P1}}, \ldots, \mathrm{T_{P5}}, \mathrm{T_{W1}}, \ldots, \mathrm{T_{W9}}, \mathrm{T_{L1}}, \ldots, \mathrm{T_{Ln}}, \mathrm{T_{Lr1}}, \ldots, \mathrm{T_{Lrn}}\}$.

Taking Eq.(7) as an example, the design process is explained as follows. (i) the GCC is in PG3 (i.e. the energy network runs in islanded mode). (ii) the battery unit is in $\mathrm{P_{B3}}$ (i.e. stopping mode because $S_{soc}(t) < 0.4\mathrm{S_{max}}$). (iii) $0.1 \le -\Delta U_d(t) \le 0.15$, and the duration exceeds $\Delta T_1 > 0$. When the above three events (i)-(iii) occur simultaneously, ETF(TL1) is activated (i.e. becomes logic "1"). Corresponding control command is sent to the load agent by the second-level agent, and then triggers the connected transition $\mathrm{T_{L1}}$ for d_{TL1} duration to execute first-grade load shedding. The explanation for design process of other equations (8)-(18) is omitted here due to the similarity.

The designed ETFs above can execute hierarchical load shedding and hierarchical switching control. In accordance with them, the control modes of resources-grid-load-storage can be switched in a coordinated way to make full use of RERs to meet the load demand with high security.

C. THE LOCAL SWITCHING CONTROL STRATEGY

The local switching control strategy "—▷" is designed by a set of event-triggered CVFs with the following principles: (i) once a constraint is violated, the corresponding CVF is activated (i.e., becomes logic "1"); and (ii) it triggers the connected transition with the corresponding operation mode being switched.

In the battery unit, the CVFs associated with $\mathrm{T_{B3}}$-$\mathrm{T_{B6}}$ are designed as follows:

$$\begin{aligned}\mathrm{CVF}(\mathrm{T_{B3}}) = {} & \mathrm{Sgn}[\max\{(P_b(t) - P_{\mathrm{b.max}}), 0\}] \\ & \mathrm{Sgn}[\max\{(0.4\mathrm{S_{max}} - S_{SOC}(t)), 0\}] \\ & \times\Phi(\mathrm{T_{B3}})\end{aligned} \tag{19}$$

$$\begin{aligned}\mathrm{CVF}(\mathrm{T_{B4}}) = {} & \mathrm{Sgn}[\max\{(S_{\mathrm{SOC}}(t) - 0.4\mathrm{S_{max}}), 0\}] \\ & \mathrm{Sgn}[\max\{(S_{\mathrm{SOC}}(t - \Delta\tau_1) - 0.4\mathrm{S_{max}}), 0\}] \\ & \times\Phi(\mathrm{T_{B4}})\end{aligned} \tag{20}$$

$$\begin{aligned}\mathrm{CVF}(\mathrm{T_{B5}}) = {} & \mathrm{Sgn}[\max\{(S_{\mathrm{SOC}}(t) - 0.9\mathrm{S_{max}}), 0\}] \\ & \mathrm{Sgn}[\max\{(S_{\mathrm{SOC}}(t - \Delta\tau_2) - 0.9\mathrm{S_{max}}), 0\}] \\ & \times\Phi(\mathrm{T_{B5}})\end{aligned} \tag{21}$$

$$\begin{aligned}\mathrm{CVF}(\mathrm{T_{B6}}) = {} & \mathrm{Sgn}[\max\{(0.9\mathrm{S_{max}} - S_{SOC}(t)), 0\}] \\ & \mathrm{Sgn}[\max\{(0.9\mathrm{S_{max}} - S_{SOC}(t - \Delta\tau_3)), 0\}] \\ & \times\Phi(\mathrm{T_{B6}})\end{aligned} \tag{22}$$

where $P_{\mathrm{b}}(t)$ is the battery power, and $P_{\mathrm{b,max}}$ is its maximum limiting value; $S_{\mathrm{soc}}(t)$ is the state of charge, and $0.4\mathrm{S_{max}}$ and

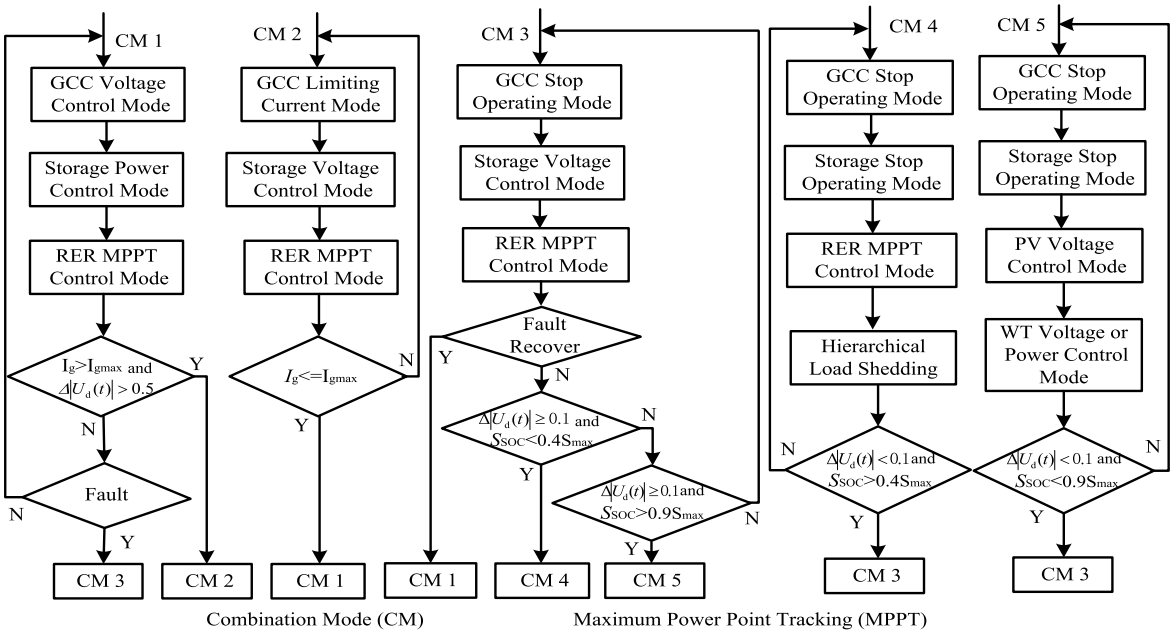

FIGURE 3. Process of implementing MAS based event-triggered hybrid controls.

$0.9S_{max}$ are defined as its minimum and maximum state of charge; $\Delta\tau_1$ is the duration when $S_{soc}(t)$ rises above $0.4S_{max}$, $\Delta\tau_2$ is the duration when $S_{soc}(t)$ rises above $0.9S_{max}$, and $\Delta\tau_3$ is the duration when $S_{soc}(t)$ drops below $0.9S_{max}$.

In the PV unit, the CVFs associated with TP3-TP5 are designed as follows:

$$\mathrm{CVF}(\mathrm{T_{P3}}) = \mathrm{Sgn}[\max\{\mathrm{C} - G_{\mathrm{ing}}(t)), 0\}]\,\Phi(\mathrm{T_{P3}}) \quad (23)$$

$$\mathrm{CVF}(\mathrm{T_{P4}}) = \mathrm{Sgn}[\max\{G_{\mathrm{ing}}(t) - \mathrm{C}), 0\}]\,\Phi(\mathrm{T_{P4}}) \quad (24)$$

$$\mathrm{CVF}(\mathrm{T_{P5}}) = \mathrm{Sgn}[\max\{\mathrm{C} - G_{\mathrm{ing}}(t)), 0\}]\,\Phi(\mathrm{T_{P5}}) \quad (25)$$

where $G_{\mathrm{ing}}(t)$ is the incident irradiance with the threshold value C.

In the WT unit, the CVFs associated with on TW3- TW7 are designed as follows:

$$\mathrm{CVF}(\mathrm{T_{W3}}) = \mathrm{Sgn}[\max\{v_{ci} - v(t)), 0\}]\,\Phi(\mathrm{T_{W3}}) \quad (26)$$

$$\mathrm{CVF}(\mathrm{T_{W4}}) = \mathrm{Sgn}[\max\{(v(t) - v_{ci}), 0\}]\,\Phi(\mathrm{T_{W4}}) \quad (27)$$

$$\mathrm{CVF}(\mathrm{T_{W5}}) = \mathrm{Sgn}[\max\{(v(t) - v_{co}), 0\}]\,\Phi(\mathrm{T_{W5}}) \quad (28)$$

$$\mathrm{CVF}(\mathrm{T_{W6}}) = \mathrm{Sgn}[\max\{v_{co} - v(t)), 0\}]\,\Phi(\mathrm{T_{W6}}) \quad (29)$$

$$\mathrm{CVF}(\mathrm{T_{W7}}) = \mathrm{Sgn}[\max\{v_{ci} - v(t)), 0\}]\,\Phi(\mathrm{T_{W7}}) \quad (30)$$

where $v(t)$ is the wind speed; v_{ci} is the cut-in wind speed; v_{co} is the cut-off wind speed.

Taking Eq.(20) as an example, the design process is explained as follows: when the $S_{soc}(t)$ of the battery rises above $0.4S_{max}$ for $\Delta\tau_1$ duration, $\mathrm{CVF}(\mathrm{T_{B4}})$ is activated (i.e. becomes logic "1"), and then triggers the connected transition $\mathrm{T_{B4}}$ for d_{TB4} duration. As a result, the control mode of the battery is switched from $\mathrm{P_{B3}}$ to $\mathrm{P_{B1}}$. The explanations for design process of other equations (21)-(30) are omitted here due to similarity.

According to the designed CVFs, the control mode of each DER unit can be switched intelligently in accordance with the constraint conditions to ensure operative security.

D. THE DISTRIBUTED DYNAMICAL CONTROL STRATEGY

For the GCC and all DER units, corresponding to all operation modes (except for stopping mode), the distributed dynamical control strategies "⋯▷" are also presented. Several advanced design methods regarding the dynamical control strategies have been proposed in the previous works of authors [8], [15], [16]. Due to the page limitation, the detailed design process will not be given in this paper.

Corresponding to Fig. 1, the process of implementing an MAS based event-triggered hybrid control scheme is briefly described in Fig. 3.

V. SIMULATION RESULTS

In this section, we provide simulation results for the following cases:

Case 1: the energy internet in a grid-connected mode suffers from frequent load variations;

Case 2: the energy internet in an islanded mode suffers from a fault. At some point, the battery is not able to control the DC bus voltage because $S_{\mathrm{SOC}} \geq 0.9S_{max}$. Thus, the RER units have to execute hierarchical switching control to maintain the voltage; and

Case 3: the energy internet is also in an islanded mode because of a fault. At some point, the battery is not able to control the DC bus voltage because $S_{\mathrm{SOC}} \leq 0.4S_{max}$. Thus, the load remand side has to implement hierarchical load shedding.

To estimate the control performance by using comparative results, the following control schemes are used: (i) the proposed control scheme in this paper; (ii) the control scheme in [12]; and (iii) the fuzzy-logic-rule-based control scheme similar to [11].

A. CASE 1

By using an MAS based hybrid control scheme in this paper, the active power of the resource-grid-load-storage units is given in Fig. 4 (a). The main operating events are listed in Table 1. By using the three different control schemes, the DC bus voltage performance of the energy internet is shown in Fig. 4 (b)-(d), respectively.

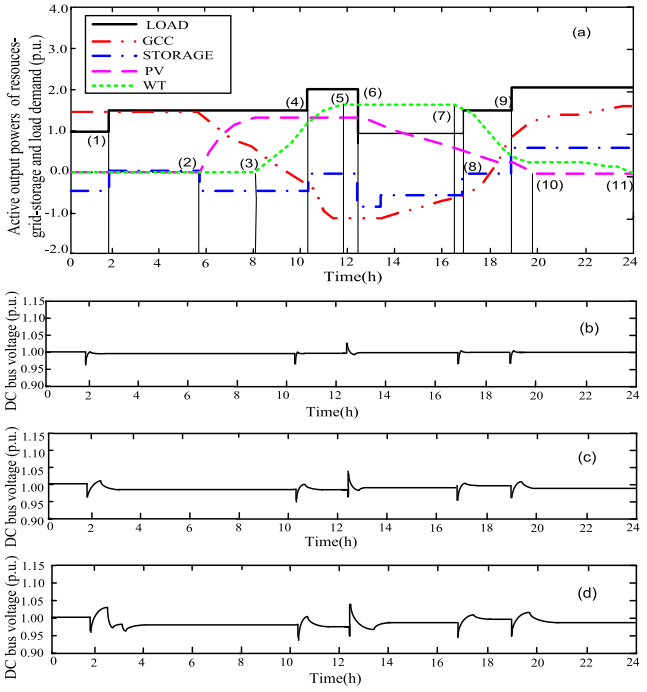

FIGURE 4. Control performance in case 1 (a) the active powers of resource-grid-load-storage; (b) the DC bus voltage in control (1); (c) the DC bus voltage in control (2); (d) the DC bus voltage in control (3).

From Fig. 4 (a) and Table 1, it can be deduced that the load variations do not result in the GCC current reaching its limitation value. Thus, the GCC unit always runs in the voltage control (VC) mode, and the battery unit always in the power control (PC) mode. In this case, the first-level agent only dynamically controls the GCC to guarantee the DC bus voltage performance of the energy internet, without implementing the switching control of GCC. The second-level agent also does not implement the coordinated switching control. The storage unit agent frequently regulates charging and discharging states of the storage device to ensure the balance between the power supply and the load demand. Only PV and WT unit agents implement local switching control in accordance with the incident irradiance and the wind speed.

From Fig. 4 (b)-(d), it can be seen that, at several instants of load variations, though the different control schemes are able to control the DC bus voltage into the secure range of [0.95, 1.05], the voltage under the proposed control scheme in this paper has the smallest fluctuations than the other two schemes. The comparative results imply that the proposed control scheme in this paper can provide the better voltage performance in the case of suffering from the load variations.

B. CASE 2

At the instant of $t = 3$h, a three-phase short circuit fault occurs in the transmission line between the energy network and the main grid. By means of the proposed control scheme in this paper, the active power of the resource-grid- load-storage is given in Fig. 5(a). The main operating events are listed in Table II. By using the three different control schemes, the DC bus voltage of the energy internet is given in Fig. 5 (b)-(d), respectively.

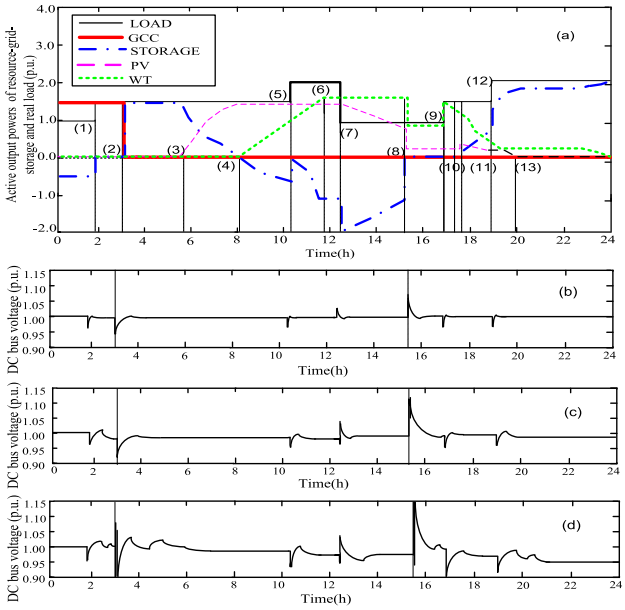

FIGURE 5. Control performance in case 2 (a) the active powers of resource-grid-load-storage; (b) the DC bus voltage in control (1); (c) the DC bus voltage in control (2); (d) the DC bus voltage in control (3).

In Table 2, there are two important instants: (i) at $t = 3$h, the first-level agent switches the GCC unit from the VC mode to the stopping mode because of the fault, resulting in the energy internet running in an islanded mode. Almost at the same time, the storage unit is switched from the PC mode to the VC mode by the control command from the second-level agent; (ii) at $t = 13.10$h, the storage unit is switched to the stopping mode by its unit agent because $S_{\mathrm{SOC}} \geq 0.9\mathrm{S}_{\mathrm{max}}$. To control the bus voltage, the PV unit is switched from the maximum power point tracking (MPPT) control mode to the VC mode by the control command from the second-level agent. However, the DC bus voltage is still very high. Later, the WT is also switched to the VC mode, and again to the PC mode 1 by the second-level agent. At the above two important instants, the multi-agent based hybrid control

TABLE 1. Main Operating Events in case 1.

Events	Times	Agent	Operating condition variations
(1)	1.50	Load agent	Load increases; GCC still runs in VC mode; the storage unit still operates in PC mode, but it is adjusted from charging state to stopping state.
(2)	5.45	PV unit agent;	PV unit is switched from stopping mode to maximum MPPT control mode; the storage unit still operates in PC mode, but it is adjusted from stopping state to charging state.
(3)	8.05	WT unit agent	WT unit is switched from stopping mode to MPPT control mode.
(4)	10.20	Load agent	Load increases; the storage unit still operates in PC mode, but it is adjusted from charging state to stopping state.
(5)	11.45	WT unit agent	WT unit is switched from MPPT control mode to PC mode 1.
(6)	12.25	Load agent	Load decreases; the battery unit still operates in PC mode, but it is adjusted from stopping state to charging state.
(7)	16.30	WT unit agent	WT unit is switched to from PC mode 1 MPPT control mode.
(8)	17.00	Load agent	Load increases; the battery unit still operates in PC mode, but it is adjusted from charging state to stopping state.
(9)	18.55	Load agent	Load increases.
(10)	19.50	PV unit agent	PV unit is switched from MPPT control mode to stopping mode.
(11)	20.00	WT unit agent	WT unit is switched from MPPT control mode to stopping mode.

can implement hierarchical switching among resource-grid-storages in a coordinated way.

From Fig. 5(b)-(d), it can be seen that even at two important instants, the proposed control scheme in this paper rapidly control the DC bus voltage into the secure range of [0.95, 1.05]. Though the second control scheme is also able to guarantee the voltage in the secure range, the voltage presents larger fluctuations. However, the third control scheme is ultimately not able to control the DC bus voltage into the secure range. The comparative results show that the proposed control scheme in this paper presents the better voltage performance even when the energy internet suffers from the large disturbance.

C. CASE 3

Similarly, at $t = 3$h, a three-phase short circuit fault is detected, resulting in the energy internet operating in an islanded mode. By using the proposed control scheme in this paper the active power of resource-grid-load-storage is shown in Fig. 6(a). The main operating events in Case 3 are very different from the ones in Case 2 because of different loads. Particularly, at $t = 20.20$h, the storage unit is switched to the stopping mode by its unit agent because of $S_{SOC} \leq 0.4S_{max}$. At the moment, the PV has stopped operating, and the WT outputs power very small. To ensure the security of the bus voltage, the second-level agent sends control command to the load agent to implement the first-level load shedding. However, after some time, the bus voltage still cannot rise into the secure range, and thus, the load agent implements the second-level load shedding. The DC bus voltage of the energy internet is given in Fig. 6(b)-(d), respectively, corresponding to three different control schemes.

TABLE 2. Main Operating Events in case 2.

Events	Times	Agent	Operating condition variations
(1)	1.50	Load agent	Load increases; GCC still runs in VC mode; the battery unit still operates in PC mode, but it is adjusted from charging state to stopping state.
(2)	3.00	first-level agent and second-level agent;	A fault occurs; the GCC unit is switched from VC mode to stopping mode; the battery unit is switched from PV mode to VC mode.
(3)	5.45	PV unit agent	PV unit is switched to MPPTC mode from stopping mode.
(4)	8.05	WT unit agent	WT unit is switched from stopping mode to MPPT control mode.
(5)	10.20	Load agent	Load increases.
(6)	11.45	WT unit agent	WT unit is switched from MPPT control mode to PC mode 1.
(7)	12.25	Load agent	Load decreases.
(8)	13.10	Storage unit agent and second-level agent	The storage unit is switched from VC mode to stopping mode because of $S_{SOC} \geq 0.9S_{max}$; afterwards, the PV unit is switched from MPPT control mode to VC mode; later, the WT unit is switched form PC mode 1 to VC mode.
(9)	16.50	Second-level agent and load agent	Load increases; the WT unit is switched form VC mode to MPPT control mode.
(10)	17.15	Second-level agent	The storage unit is switched from stopping mode to VC mode because of $S_{SOC} < 0.9S_{max}$.
(11)	17.40	Second-level agent	PV unit is switched from VC mode to MPPT control mode.
(12)	18.50	Load agent	Load increases.
(13)	20.00	PV unit agent	PV unit is switched from MPPT control mode to stopping mode.

TABLE 3. Description of discrete places.

Discrete Places	Description
P_{G1}	Voltage control (VC) mode of the GCC
P_{G2}	Power control (PC) mode of the GCC
P_{G3}	Stopping mode of the GCC
P_{B1},P_{B2}	VC mode and PC mode of the storage unit, respectively
P_{B3}	Stopping mode because $S_{SOC} \leq 0.4S_{max}$
P_{B4}	Stopping mode because $S_{SOC} \geq 0.9S_{max}$
P_{P1}	Maximum power point tracking (MPPT) control mode
P_{P2}, P_{P3}	VC mode of and stopping mode the PV unit, respectively
P_{W1},P_{W2}	VC mode and MPPT mode of the WT unit, respectively
P_{W3}, P_{W4}	Stopping mode and PC mode1of the WT unit, respectively
P_{W5}	PC mode 2 by regulating turn pitch angle
P_{L1}	Normal operating mode of the load demand side
P_{L2}	First-level load shedding mode
P_{L3}	Second-level load shedding mode
$P_{L(n+1)}$	Nth-level load shedding mode

From Fig. 6 (b)-(d), it can be observed that even at $t = 20.20$h, the proposed control scheme in this paper rapidly restores the DC bus voltage. The second control scheme results in larger voltage fluctuations. The third control scheme is ultimately not able to control the DC bus voltage into the secure range of [0.95, 1.05]. The comparative results show that the proposed control scheme in this paper effectively implements the hierarchical load shedding so that the energy internet can meet load with high voltage security in an islanded mode.

TABLE 4. Description of discrete transitions.

Discrete Transition	Description
T_{G1}	Switch the GCC unit from VC mode to PC mode
T_{G2}	Switch the GCC unit from PC mode to VC mode
T_{G3}	Switch the GCC unit from stopping mode to VC mode
T_{G4}	Switch the GCC unit from PC mode to stopping mode
T_{B1}	Switch the storage unit from VC mode to PC mode
T_{B2}	Switch the storage unit from VC mode to PC mode
T_{B3}	Switch the storage unit from VC mode to stopping mode because of $S_{SOC} \leq 0.4S_{max}$
T_{B4}	Switch the storage unit to VC mode from stopping mode because $S_{SOC}>0.4S_{max}$
T_{B5}	Switch the storage unit to stopping mode from VC mode because $S_{SOC} \geq 0.9S_{max}$
T_{B6}	Switch the storage unit to VC mode from stopping mode because $S_{SOC} <0.9S_{max}$
T_{P1}	Switch the PV unit from VC mode to MPPT control mode
T_{P2}	Switch the PV unit from MPPT control mode to VC mode
T_{P3}	Switch the PV unit from MPPT mode to stopping mode
T_{P4}	Switch the PV unit to MPPT mode from stopping mode
T_{P5}	Switch the PV unit from VC mode to stopping mode
T_{W1}	Switch the WT unit from MPPTC mode to VC mode
T_{W2}	Switch the WT unit from VC mode to MPPT mode
T_{W3}	Switch the WT unit from MPPT mode to stopping mode
T_{W4}	Switch the WT unit from stopping mode to MPPT mode
T_{W5}	Switch the WT unit from MPPT mode to PC mode1
T_{W6}	Switch the WT unit from PC mode1 to MPPT mode
T_{W7}	Switch the WT unit to stopping mode from VC mode
T_{W8}	Switch the WT unit from VC mode to PC mode 2
T_{W9}	Switch the WT unit from PC mode 2 to MPPT mode
T_{L1}	Implement first-level load shedding
T_{L2}	Implement second-level load shedding
T_{Ln}	Implement nth-level load shedding
T_{Lr1}	Restore load form first-level load shedding
T_{Lr2}	Restore load form second-level load shedding
T_{Lrn}	Restore load form Nth-level load shedding

TABLE 5. Description of differential places.

Differential Places	Description
P_{Gf} …P_{Lf}	Continuous dynamics of in different control mode

TABLE 6. Description of differential transitions.

Differential Transitions	Description
T_{G1f} , T_{G2f}	Dynamical VC and PC of the GCC unit respectively
T_{B1f}, T_{B2f}	Dynamical VC and PC of the storage unit respectively
T_{P1f} , T_{P2f}	Dynamical VC and MPPT of the PV unit respectively
T_{W1f} , T_{W2f}	Dynamical VC and MPPTC of the WT unit respectively
T_{W3f} , T_{W4f}	Dynamic PC 1 and PC 2 of the WT unit respectively
T_{L1f}	Dynamic controls of the load demand side
T_{L2f}, T_{L3f}	Dynamic controls in different-level load shedding

VI. CONCLUSION

This paper has developed an MAS based event-triggered hybrid control scheme, by which the energy internet can make full use of RERs to meet load demand with high security. Four types of event-triggered hybrid control strategies are firstly designed as ETFs or CVFs, which are fully dependent on the logical relationship between the resource-grid-load-storage. Based on these control strategies, MAS can then be used to implement hierarchical hybrid control in a coordinated way.

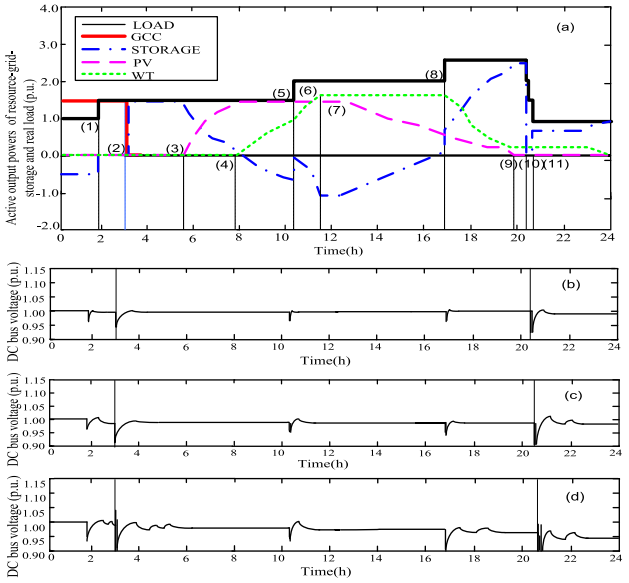

FIGURE 6. Event-triggered switching control performance in case 3 (a) the active powers of resource-grid-load-storage; (b) the DC bus voltage in control scheme (i); (c) the DC bus voltage in control scheme (ii); (d) the DC bus voltage in control scheme (iii).

In comparison with the simulation results of some existing control schemes, it is shown that the proposed hybrid control scheme can provide better voltage performance.

REFERENCES

[1] X. Yu, X. She, X. Ni, and A. Q. Huang, "System integration and hierarchical power management strategy for a solid-state transformer interfaced microgrid system," *IEEE Trans. Power Electron.*, vol. 29, no. 8, pp. 4414–4425, Aug. 2014.

[2] A. Hajizadeh and M. A. Golkar, "Intelligent power management strategy of hybrid distributed generation system," *Int. J. Elect. Power Energy Syst.*, vol. 29, no. 10, pp. 783–795, Dec. 2007.

[3] K. Wang *et al.*, "A survey on energy Internet: Architecture, approach, and emerging technologies," *IEEE Syst. J.*, to be published, doi: 10.1109/JSYST.2016.2639820.

[4] C.-X. Dou, D.-L. Liu, X.-B. Jia, and F. Zhao, "Management and control for smart microgrid based on hybrid control theory," *Electr. Power Compon. Syst.*, vol. 39, pp. 813–832, May 2011.

[5] H. Jiang, K. Wang, Y. Wang, M. Gao, and Y. Zhang, "Energy big data: A survey," *IEEE Access*, vol. 4, pp. 3844–3861, 2016.

[6] Q. Sun, R. Han, H. Zhang, J. Zhou, and J. M. Guerrero, "A multiagent-based consensus algorithm for distributed coordinated control of distributed generators in the energy Internet," *IEEE Trans. Smart Grid*, vol. 6, no. 6, pp. 3006–3019, Nov. 2015.

[7] T. Zhou and B. Francois, "Energy management and power control of a hybrid active wind generator for distributed power generation and grid integration," *IEEE Trans. Ind. Electron.*, vol. 58, no. 1, pp. 95–104, Jan. 2011.

[8] J. M. Guerrero, J. C. Vasquez, J. Matas, L. G. de Vicuna, and M. Castilla, "Hierarchical control of droop-controlled AC and DC microgrids—A general approach toward standardization," *IEEE Trans. Ind. Electron.*, vol. 58, no. 1, pp. 158–172, Jan. 2011.

[9] Z. Jun, L. Junfeng, W. Jie, and H. W. Ngan, "A multi-agent solution to energy management in hybrid renewable energy generation system," *Renew. Energy*, vol. 36, no. 5, pp. 1352–1363, May 2011.

[10] J. Lagorse, D. Paire, and A. Miraoui, "A multi-agent system for energy management of distributed power sources," *Renew. Energy*, vol. 35, no. 1, pp. 174–182, 2010.

[11] J. Lagorse, M. G. Simoes, and A. Miraoui, "A multiagent fuzzy-logic-based energy management of hybrid systems," *IEEE Trans. Ind. Appl.*, vol. 45, no. 6, pp. 2123–2129, Nov./Dec. 2009.

[12] C.-X. Dou, B. Liu, and J. M. Guerrero, "Event-triggered hybrid control based on multi-agent system for microgrids," *IET Generat., Transmiss. Distrib.*, vol. 8, no. 12, pp. 1987–1997, Dec. 2014.

[13] V. K. Paruchuri, A. Davari, and A. Feliachi, "Hybrid modeling of power system using hybrid Petri nets," in *Proc. Southeastern Symp. Syst. Theory*, Mar. 2005, pp. 221–224.

[14] J. Sun, S.-Y. Qin, and Y.-H. Song, "Fault diagnosis of electric power systems based on fuzzy Petri nets," *IEEE Trans. Power Syst.*, vol. 19, no. 4, pp. 2053–2059, Nov. 2004.

[15] J. M. Guerrero, J. C. Vásquez, J. Matas, M. Castilla, and L. G. de Vicuña, "Control strategy for flexible microgrid based on parallel line-interactive UPS systems," *IEEE Trans. Ind. Electron.*, vol. 56, no. 3, pp. 726–736, Mar. 2009.

[16] C.-X. Dou, B. Liu, and D. J. Hill, "Hybrid control for high-penetration distribution grid based on operational mode conversion," *IET Generat., Transmiss. Distrib.*, vol. 7, no. 7, pp. 700–708, Jul. 2013.

CHUNXIA DOU received the B.S. and M.S. degrees in automation from Northeast Heavy Machinery Institute, Qiqihaer, China, in 1989 and 1994, respectively, and the Ph.D. degree from the Institute of Electrical Engineering, Yanshan University, Qinhuangdao, China, in 2005. In 2010, she joined the Department of Engineering, Peking University, Beijing, China, where she was a Post-Doctoral Fellow for two years. Since 2005, she has been a Professor with the Institute of Electrical Engineering, Yanshan University. Her current research interests include multi-agent-based control, event-triggered hybrid control, distributed coordinated control, and multi-mode switching control and their applications in power systems, microgrids, and smart grids.

DONG YUE (SM'08) received the Ph.D. degree from South China University of Technology, Guangzhou, China, in 1995. He is currently a Professor and the Dean of the Institute of Advanced Technology, Nanjing University of Posts and Telecommunications, and also a Changjiang Professor with the Department of Control Science and Engineering, Huazhong University of Science and Technology. He has published more than 100 papers in international journals, domestic journals, and international conferences. His research interests include the analysis and synthesis of networked control systems, multi-agent systems, optimal control of power systems, and Internet of Things. He is currently an Associate Editor of the IEEE Control Systems Society Conference Editorial Board and also an Associate Editor of the IEEE TRANSACTIONS ON NEURAL NETWORKS AND LEARNING SYSTEMS, the *Journal of the Franklin Institute*, and the *International Journal of Systems Science*.

QING-LONG HAN (M'09–SM'13) received the B.Sc. degree in mathematics from Shandong Normal University, Jinan, China, in 1983, and the M.Sc. and Ph.D. degrees in control engineering and electrical engineering from East China University of Science and Technology, Shanghai, China, in 1992 and 1997, respectively.

From 1997 to 1998, he was a Post-Doctoral Researcher Fellow with the Laboratoire d'Automatique et d'Informatique Industielle (currently Laboratoire d'Informatique et d'Automatique pour les Systèmes), Ecole Supérieure d'Ingénieurs de Poitiers (currently Ecole Nationale Supérieure d'Ingénieurs de Poitiers), Université de Poitiers, France. From 1999 to 2001, he was a Research Assistant Professor with the Department of Mechanical and Industrial Engineering, Southern Illinois University at Edwardsville, USA. From 2001 to 2014, he was a Laureate Professor, the Associate Dean (Research and Innovation) with the Higher Education Division, and the Founding Director of the Centre for Intelligent and Networked Systems with Central Queensland University, Australia. From 2014 to 2016, he was a Deputy Dean (Research), with Griffith Sciences, and a Professor with the Griffith School of Engineering, Griffith University, Australia. In 2016, he joined Swinburne University of Technology, Australia, where he is currently a Pro Vice-Chancellor (Research Quality) and a Distinguished Professor. His research interests include networked control systems, neural networks, time-delay systems, multi-agent systems, and complex systems.

Prof. Han was appointed as a Chang Jiang (Yangtze River) Scholar Chair Professor by the Ministry of Education, China, in 2010. He is one of The World's Most Influential Scientific Minds: 2014–2016. He is a highly cited Researcher in Engineering according to Thomson Reuters.

JOSEP M. GUERRERO (S'01–M'04–SM'08–F'15) received the B.S. degree in telecommunications engineering, the M.S. degree in electronics engineering, and the Ph.D. degree in power electronics from Technical University of Catalonia, Barcelona, in 1997, 2000, and 2003, respectively. Since 2011, he has been a Full Professor with the Department of Energy Technology, Aalborg University, Denmark, where he is responsible for the Microgrid Research Program. Since 2012, he has been a Guest Professor with the Chinese Academy of Sciences and Nanjing University of Aeronautics and Astronautics; since 2014, he has been the Chair Professor with Shandong University, China; and since 2015, he has been a Distinguished Guest Professor with Hunan University, China. His research interests focus on different microgrid aspects, including power electronics, distributed energy-storage systems, hierarchical and cooperative control, energy management systems, and optimization of microgrids and islanded minigrids. He is currently focused on maritime microgrids for electrical ships, vessels, ferries, and seaports.

Prof. Guerrero is an Associate Editor of the IEEE TRANSACTIONS ON POWER ELECTRONICS, the IEEE TRANSACTIONS ON INDUSTRIAL ELECTRONICS, and the *IEEE Industrial Electronics Magazine*, and an Editor of the IEEE TRANSACTIONS ON SMART GRID and the IEEE TRANSACTIONS ON ENERGY CONVERSION. He has been a Guest Editor of the IEEE TRANSACTIONS ON POWER ELECTRONICS SPECIAL ISSUES: POWER ELECTRONICS FOR WIND ENERGY CONVERSION AND POWER ELECTRONICS FOR MICROGRIDS; the IEEE TRANSACTIONS ON INDUSTRIAL ELECTRONICS SPECIAL SECTIONS: UNINTERRUPTIBLE POWER SUPPLIES SYSTEMS, RENEWABLE ENERGY SYSTEMS, *Distributed Generation and Microgrids*, and *Industrial Applications and Implementation Issues of the Kalman Filter*; and the IEEE TRANSACTIONS ON SMART GRID SPECIAL ISSUE ON SMART DC DISTRIBUTION SYSTEMS. He was the Chair of the Renewable Energy Systems Technical Committee of the IEEE Industrial Electronics Society. He received the best paper award of the IEEE TRANSACTIONS ON ENERGY CONVERSION from 2014–2015. In 2014–2015, he was awarded by Thomson Reuters as a Highly Cited Researcher, and in 2015, he was elevated as an IEEE fellow for his contributions on distributed power systems and microgrids.